HHS Public Access

Author manuscript

Lab Chip. Author manuscript; available in PMC 2017 April 26.

Published in final edited form as:

Lab Chip. 2016 April 26; 16(9): 1579–1586. doi:10.1039/c6lc00001k.

Elastomeric Free-Form Blood Vessels for Interconnecting Organs on Chip Systems †

Weijia Zhang[1,2,3,†], **Yu Shrike Zhang**[1,2,4,†], **Syeda Mahwish Bakht**[1,2,5,†], **Julio Aleman**[1,2], **Su-Ryon Shin**[1,2,4], **Kan Yue**[1,2], **Marco Sica**[1,2,6], **João Ribas**[1,2,7,8], **Margaux Duchamp**[1,2,9], **Jie Ju**[1,2], **Ramin Banan Sadeghian**[1,2,10], **Duckjin Kim**[1,2], **Mehmet Remzi Dokmeci**[1,2,4], **Anthony Atala**[11], and **Ali Khademhosseini**[1,2,9,12,13,*]

[1]Biomaterials Innovation Research Center, Division of Biomedical Engineering, Department of Medicine, Brigham and Women's Hospital, Harvard Medical School, Cambridge, MA 02139, USA [2]Harvard-MIT Division of Health Sciences and Technology, Massachusetts Institute of Technology, Cambridge, MA 02139, USA [3]Shanghai Ocean University, Shanghai, 201306, P.R. China [4]Wyss Institute for Biologically Inspired Engineering, Harvard University, Cambridge, MA 02139, USA [5]COMSATS Institute of Information and Technology, Islamabad 45550, Pakistan [6]Department of Biomedical Engineering, Politecnico di Torino, Torino 10129, Italy [7]Doctoral Programme in Experimental Biology and Biomedicine, Center for Neuroscience and Cell Biology, Institute for Interdisciplinary Research, University of Coimbra, Coimbra 3030-789, Portugal [8]Biocant — Biotechnology Innovation Center, Cantanhede 3060-197, Portugal [9]Department of Bioengineering, École Polytechnique Fédérale de Lausanne, Lausanne 1015, Switzerland [10]WPI-Advanced Institute for Materials Research, Tohoku University, Sendai 980-8578, Japan [11]Wake Forest Institute for Regenerative Medicine, Winston-Salem, NC 27101, USA [12]Department of Bioindustrial Technologies, College of Animal Bioscience and Technology, Konkuk University, Seoul 143-701, Republic of Korea [13]Department of Physics, King Abdulaziz University, Jeddah 21569, Saudi Arabia

Abstract

Conventional blood vessel-on-a-chip models are typically based on microchannel-like structures enclosed within bulk elastomers such as polydimethylsiloxane (PDMS). However, these bulk vascular models largely function as individual platforms and exhibit limited flexibility particularly when used in conjunction with other organ modules. Oftentimes lengthy connectors and/or tubes are still needed to interface multiple chips, resulting in a large waste volume counterintuitive to the miniaturized nature of the organs-on-chips. In this work, we report the development of a novel form of vascular module based on PDMS hollow tubes, which closely emulates the morphology

†Electronic Supplementary Information (ESI) available: [details of any supplementary information available should be included here]. See DOI: 10.1039/c000000x/

*Corresponding author: alik@bwh.harvard.edu.
†W.Z., Y.S.Z., and S.M.B. contributed equally.

Author Contributions

W.Z. and Y.S.Z. designed and performed the experiments, analyzed the data, and wrote the manuscript; S.M.B, J.A., K.Y., M.S., J.R., J.J., M.D., and R.B.S. performed the experiments and analyzed the data; S.R.S. participated in the design of the experiments; M.R.D. and A.A. provided technical guidance and revised the manuscript; A.K. supervised the project and revised the manuscript.

and properties of the human blood vessels to integrate multiple organ-on-chips. Specifically, we present two templating strategies to fabricate hollow PDMS tubes with adjustable diameters and wall thicknesses, where metal rods or airflow were employed as the inner templates, while plastic tubes were used as the outer template. The PDMS tubes could then be functionalized by human umbilical vein endothelial cells (HUVECs) in their interior surfaces to further construct the elastomeric biomimetic blood vessels. The endothelium developed biofunctionality as demonstrated by the expression of endothelial biomarker CD31 as well as dose-dependent responses in the secretion of von Willebrand factor and nitric oxide upon treatment with pharmaceutical compounds. We believe that, with their clear advantages including high optical transparency, gas permeability, and tunable elasticity matching those of native blood vessels, these free-form PDMS vascular modules can supplement the bulk vascular organoids and likely replace the inert plastic tubes in integrating multiple organoids into a single microfluidic circuitry.

Introduction

Multi-organ-on-chips platforms that mimic human organ functions and interactions are emerging as improved model systems for studying diseases as well as assessing the effects of drug candidates, toxins, and biological agents on the body.[1–8] Currently, the gold standards in these applications rely on animal models and *in vitro* cell cultures, both of which are limited in their efficacy. Animal models are associated with high costs and uncertain interpretation of testing results due to interspecies difference.[9, 10] The human pharmacokinetics and toxicology are poorly predicable through the use of animal models. On the other hand, static cultures of human cells, although inexpensive, fail to fully model the intricate *in vivo* microenvironments of many tissues/organs.[8, 9, 11, 12] By merging advances in microfabrication, microfluidic technology, and tissue engineering, a novel *in vitro* microphysiology system, also known as organs-on-chip, has recently been introduced to the field, aiming to provide new options for better mimicking organ functions on miniaturized devices.[1–9, 11, 12] These systems include dynamic fluid flows and thereby prolonged organoid cultures may be achieved. More importantly, multiple microscale human organs-on-chip models can be integrated in a single microfluidic circuitry to allow for inter-organoid interactions and thus much closer recapitulation of the human physiology.

The conventional lithography techniques allow us to fabricate microchannels with well-defined geometries simulating the vascular network, typically enclosed in bulk elastomers or plastics. These microchannels may further be endothelialized to introduce the biological functions that mimic the blood vessels. Over the past decades, a large number of on-chip vascular devices have been intensively explored and developed.[13–18] However, chip-based bulk vascular constructs are not suitable for integration with multiple organs-on-chip systems because they introduce at least two levels of complexity. First, the sizes of these chip-based vascular models almost equal those of individual organoids. Using them as the connecting components will inevitably induce biased scaling, which in addition, cannot be conveniently adjusted with pre-existing molds.[3] Second, the bulky volume of these vascular chips cannot fit the purpose of connecting multiple organoid modules, particularly when more than one connections are required among the organoids to be integrated. To this end,

bioinert connectors and/or plastic tubes are often used, leading to wasted dead volumes counterintuitive to the miniaturized nature of the organs-on-chips devices.

In contrast to the majority of the existing vascular chips or passive tube connections, here we report the development of a simple form of elastomeric biomimetic blood vessels closely mimicking the physio-anatomical properties of those *in vivo*, for integrating multiple organs on chips. Specifically, we adopted two templating strategies where commercial plastic tubes were used as the outer molds and metal rods or air flow as the inner templates, to fabricate hollow polydimethylsiloxane (PDMS) tubes with adjustable diameters and wall thicknesses. Biological functions were further introduced by coating a confluent layer of human umbilical vein endothelial cells (HUVECs) in the interiors of the PDMS tubes to mimic the endothelium lining of the blood vessels. The endothelium developed biofunctionality as demonstrated by expression of endothelial biomarker CD31 as well as dose-dependent responses in the secretion of von Willebrand factor and nitric oxide upon treatment with pharmaceutical compounds. We believe that, these elastomeric biomimetic vessels may find widespread applications in the fields of microfluidics and organs-on-chips by supplementing the bulk vascular modules and replacing the passive plastic tubes in integrating multiple organoids into a single microfluidic circuitry (Figure 1).

Experimental Section

A. Hard templating approach for fabrication of PDMS tubes

In the hard templating approach, plastic (polyurethane or polyethylene) tubes with inner diameters of 2.6 mm and 0.85 mm were used as the outer templates. Metal rods with diameters of 1.27 mm, 0.64 mm, and 0.28 mm were used as the inner templates. First, the plastic tubes were pre-cut on one side. The inner surface of the tubes and the outer surface of the metal rods were pre-coated with a thin layer of mineral oil to ensure that the templating tubes and rods could be easily removed from the fabricated PDMS tubes. Second, the PDMS pre-polymer mixture (weight ratio of monomer to curing agent: 10-1 or 20-1) was perfused into the plastic tubes. Metal rods were then inserted into the center of the liquid PDMS precursor. PMMA holders were prepared by a laser cutter and used to fix the relative positions of plastic tubes and metal rods. The PMMA holders were precisely engraved to fix tubes and metal rods/needles with different diameters. The PDMS was then cured in the oven at 80 °C. Afterwards, the plastic tubes and metal rods were carefully removed, and the resulting PDMS tubes were cleaned with the sodium dodecyl sulfate (SDS) detergent to remove residual mineral oil.

B. Soft templating approach for fabrication of PDMS tubes

In the soft templating approach, plastic tubes with inner diameters of 2.6 mm and 4.2 mm were used as the outer templates and were similarly treated as in the hard templating method. First, the plastic tubes were pre-cut on one side. The inner surface of tubes were pre-coated with a thin layer of mineral oil. Second, the PDMS pre-polymer mixture (weight ratio of monomer to curing agent: 10-1 or 20-1) was perfused into the plastic tubes. PMMA holders were also used to fix the position of the plastic tubes in this case. During the curing of PDMS, the airflow through the tubes was maintained constant and a small rotator was

used to allow the entire sets of PMMA holder, plastic tube, and PDMS pre-polymer mixture to rotate at approximate 200 rpm. After PDMS was cured at 80 °C, the plastic tubes were then carefully removed, and the resulting PDMS tubes were cleaned by SDS.

C. Measurement of tensile strength of PDMS

The tensile strength was measured on PDMS with different compositions as well as curing times and temperatures. PDMS sheets were fabricated by casting the PDMS precursor mixture in a PMMA mold. The dimension of PDMS sheets was 25L×6W×1.1H mm^3. To measure the tensile strength, PDMS sheets were clamped at both ends using clips. Stress-strain curves were obtained using an Instron 5542 mechanical tester. The Young's modulus was calculated as the slope of the stress-strain curve at the initial linear region (10% strain). Three samples were measured for each group.

D. Endothelialization of the PDMS tubes

HUVECs were cultured in an endothelial basal medium (EBM-2; Lonza) supplemented with endothelial growth kit (BulletKit, EGM-2; Lonza), together referred to as endothelial growth medium (EGM), and maintained at 37 °C in a humidified, 5% CO_2 incubator. The medium was changed every 2–3 days and the cells were passaged at 70% confluence. Prior to seeding HUVECs, the PDMS tubes were sterilized using 70% ethanol, air-dried for 10 min, treated by UV irritation for 30 min, and then incubated with 50 μg mL^{-1} fibronectin (Sigma-Aldrich) at room temperature for overnight. To form an endothelial monolayer, HUVECs were trypsinized and collected from the culture flask, and then re-suspended in the EGM at a density of 2×10^6 cells mL^{-1}. The fibronectin-coated PDMS tubes were perfused with the cell suspension and immediately placed back into the incubator to allow for cell attachment on their inner surfaces for 2 h. This process was repeated once with the PDMS tubes flipped upside down between the two seeding steps. The endothelialized PDMS tubes were then gently rinsed with medium to wash away loosely attached cells and maintained in perfusion cultures at a flow rate of 10 μL min^{-1} using a peristaltic pump. The media in the reservoir were collected every one or two days, centrifuged, and the supernatants were measured for endothelial biomarker endothelin-1 (ET-1) using a standard ELISA kit (Abcam).

E. Fluorescent staining of endothelial monolayers

After 7 days of culture, F-actin (Life Technologies) and CD31 (PECAM-1, Abcam) stainings were performed to investigate the effective formation of endothelial monolayers within the PDMS tubes. The cells were fixed in 4% (w/v) paraformaldehyde (Sigma-Aldrich) for 15 min and incubated in 0.1% (v/v) Triton X-100 (Sigma-Aldrich) in PBS for 15 min to permeabilize the cell membrane. Afterwards, the samples were blocked in 1% (w/v) BSA in PBS for 1 h at room temperature. To label F-actin, the samples were incubated in Alexa 488-phalloidin (1:40 dilution) in phosphate buffered saline (PBS, Life Technologies). To stain CD31, the samples were incubated in rabbit anti-CD31 primary antibody (Abcam) solution (1:50 dilution) in PBS for 1 h at room temperature and then Alexa 594 conjugated anti-rabbit secondary antibody (Life Technologies) solution (1:200 dilution) in PBS for 1 h at room temperature. The samples were finally stained with 4',6-diamidino-2-phenylindole (DAPI, Life Technologies) for the nuclei. Fluorescence images

were acquired using a fluorescence microscope (Axio Observer D1, Zeiss) and a laser scanning confocal microscope (TCS SP5, Leica).

F. Assessment of drug effects on the endothelialized PDMS tubes

A panel of drugs including anti-cancer drug doxorubicin (0-15 μg mL^{-1}), immunosuppressive drug rapamycin (0-10 μg mL^{-1}), and vasodilator medication minoxidil (0-5 μM), were used to evaluate the bioactivity of the endothelialized PDMS tubes. The media in the reservoir were collected every one or two days, centrifuged, and the supernatants were measured for endothelial biomarker von Willebrand factor (vWF) using a standard ELISA kit (Abcam). The ability of the endothelialized PDMS tubes to modulate the production levels of nitric oxide (NO) was assessed by treatment with rapamycin (10 μg mL^{-1}), amiodarone (30 μM), and acetaminophen (10 mM). Vasodilator histamine (100 μM) was used as a positive control. The one-channel free radical analyzer (TBR1025, World Precision Instruments) was used to measure the levels of NO. The sensor was placed inside a Faraday cage to avoid interferences from the environment. The NO sensor probe was inserted into the PDMS tubes, and medium was perfused at a flow rate of 2 mL h^{-1}. After the sensor signal stabilized, normal medium was replaced with medium containing the target drugs.

G. Statistics

Statistical analyses were conducted using unpaired t-tests with a size of at least 3–5 samples per group. Statistical significance was determined at $p < 0.05$.

Results and discussion

The vascular system in a human body is composed of three major classes, i.e. arteries, veins, and capillaries, which are organized in hierarchically distinct structures.[19] Healthy arteries have strong, elastic, and thick vessel walls that can resist high pressures and carry blood away from the heart. In contrast, veins have thinner walls than arteries but wider inner diameters that can recycle the blood back to the heart. Custom-designed tubes with desired diameters and wall thicknesses can be tailored to meet required applications,[20] as exemplified in a prior work where cellulose-based microtubes were used as artificial blood vessels.[21]

Specifically, we chose PDMS because this elastomer has been widely used the field due to its excellent material attributes, such as easy polymerization, optical transparency, tunable elasticity, gas permeability, water sealing capacity, biocompatibility, and inexpensiveness.[22–24] To fabricate the PDMS tubes with a range of different sizes and wall thicknesses, we developed both hard templating and soft templating approaches. The hard templating method is shown in Figure 2a. In a typical process, the PDMS precursor mixture was perfused into the space between a metal rod/needle inserted into a plastic tube. After 2 h curing at 80 °C, the templates were removed and the newly molded PDMS tubes could be recovered. The outer diameter and the wall thickness of the obtained PDMS tubes were conveniently adjustable according to the size of the templates. As shown in Figure 2c-d, plastic tubes with inner diameters ranging from 0.85 to 4.2 mm served as the outer templates

and metal rods or needles with outer diameters ranging from 0.28 to 1.27 mm were used as the inner templates. Figure 3a-c present representative photographs of the PDMS tubes fabricated by the hard templating method, which had 2.6/2.6/0.65-mm outer diameters and 1.27/0.64/0.28-mm inner diameters.

Thin-walled PDMS tubes were not easily achievable by hard templating, because thinner PDMS walls would break during the withdrawal of the central metal rods. Hence, we further introduced a soft templating method to fabricate PDMS tubes with very thin walls. Briefly, the PDMS precursor mixture was perfused into a plastic tube and placed in an oven heated at 80 °C. During the curing process, clean air was perfused as the soft template at a constant flow and the entire tube was subjected to continuous rotation against the central axis. Post curing, the plastic tubes were removed to retrieve the PDMS tubes. As shown in Figure 2d-e, PDMS tubes with 4.2/2.6-mm outer diameters and 0.5/0.3-mm wall thicknesses could be produced using the soft templating approach. In contrast to the hard templating method for generation of artery-like structures, soft templating is more suitable for fabricating PDMS tubes with thinner walls that mimic thin-walled vessels such as veins and capillaries. The wall thickness of these PDMS tubes was relatively uniform, with the difference between the thickest/thinnest locations along the circumference falling below 35%, which we believe is sufficient for their use as vascular models. It was further found that, the air flow did not significantly affect the wall thickness of the resulting PDMS tubes within the range of flow rate tested (1-10 L min^{-1}). However, the wall thickness could be more conveniently controlled by the viscosity of the PDMS prepolymer – for example, curing the PDMS perpolymer in an over at 80 °C for 5–10 min prior to coating the template roughly doubled the wall thickness of the fabricated PDMS tubes.

Supplementary Figure S1 shows a panel of PDMS tubes with drastically different ratios of diameter to wall thickness fabricate by both hard and soft templating methods. As such ratios for the blood vessels in the human blood lie in the range of 4:1 to 10:1,[19] our fabricated PDMS tubes will likely meet the physiological requirements in mimicking the full spectrum of different arteries and veins. SEM images PDMS tubes further revealed their smooth inner surfaces (Supplementary Figure S2). The maximal length of PDMS tubes fabricated by the hard templating method is largely limited by the length of the rods/needles. On the other hand, in the soft templating method, stability of the rotation during the curing determines the length of the resulting PDMS tubes. Using both methods, we were able to achieve PDMS tubes of up to 20 cm in length, which is sufficiently long for most organs-on-chip applications.

The resulting PDMS tubes were highly flexible and could be easily twisted while still remaining intact (Figure 3f-g). The capability to adjust the elasticity of the PDMS tubes raises another key advantage for their use as a viable type of vascular modules, since the elasticities of arterial and venous vessels may vary significantly. For example, elastin, which is produced by fibroblasts and smooth muscle cells in the blood vessels, renders them with a wide range of moduli in approximate range of 280–500 kPa.[25–29] We determined that, the Young's modulus of PDMS could be adjusted from 250 to 1900 kPa by simply changing the composition of the prepolymer mixture (i.e. weight ratios of the monomer to the curing agent) and the curing time (Figure 3h). Since the modulus of PDMS can be adjusted to

match that of the blood vessels, it is advantageous compared to commercial plastic tubes that usually present fixed mechanical properties (supplementary Table S1). In some diseases, such as diabetes and hyperlipidemia, blood vessels undergo dramatic hardening and thickening.[30], [31] The adjustable elasticity and wall thickness of the PDMS tubes that we have innovated can thus potentially benefit the studies on disease models and their respective drug effects, potentially expanding their applications in multi-organs-on-chips platforms.

We further demonstrated the possibility to construct the biomimetic vessels by coating the inner surface of the PDMS tubes with a layer of endothelial cells (e.g. HUVECs used in this study). PDMS surface is a suitable substrate for culturing mammalian cells because of its biological inertness and gas permeability.[32] However, native PDMS surface is unfavorable for cell attachment. Coating PDMS with bioactive proteins or hydrogels, such as fibronectin or collagen, can facilitate the attachment of cells.[33–36] In this study, the PDMS tubes were treated with UV irritation for 30 min to produce an activated polymer surface and then incubated with 50 μg mL^{-1} fibronectin solution for overnight to introduce the surface coating layer. It should be noted that, we chose to use only the thick-walled PDMS tubes fabricated from the hard templating method for following studies due to their ease of handling. Considering their similarity in the surface smoothness (Supplementary Figure S2) and material properties, we do not expect significant difference in the bioactivities of the two types of endothelialized tubes.

To form the endothelium, HUVECs were seeded into the PDMS tube coated with fibronectin. The seeded cells were allowed to attach for 2 h and then seeding was repeated. The PDMS tubes were flipped upside down between the two seeding procedures to ensure uniform cell distribution. Afterwards, the cell-bearing PDMS tubes were immersed in EGM for perfusion culture at a flow rate of 10 μL min^{-1}.

To visualize the HUVECs cells within the PDMS tubes, F-actin was stained with Alexa 488-phalloidin (green) and the nuclei were counterstained with DAPI (blue). Figure 4a-c shows representative fluorescence images of stained HUVECs in PDMS tubes with inner diameters of 0.28, 0.64, and 1.27 mm, respectively. In all cases the cells proliferated over a course of 7 days and gradually became confluent to form an intact layer of endothelium in each tube. The cell densities were then quantified against the number of nuclei (Figure 4d). HUVECs seeded within larger tubes (0.64 mm and 1.27 mm) reached higher cell densities primarily due to the relatively flatter inner surfaces of these tubes than the small tubes (0.28 mm). It should be noted that, even after the formation of the endothelial linings, these tubular constructs still maintained fully perfusable hollow lumens, as illustrated in microscopic images of the endothelium from different (apical, middle, and basal) planes (supplementary Figure S3). This feature of the endothelialized PDMS vessels enables effective transport of medium and ensures their use to integrate multiple organs-on-chips systems.

In addition, the tight endothelium coated on the interior surfaces of the PDMS tubes expressed junction biomarker CD31 (Figure 4e-f), indicative of the functional recapitulation of their *in vivo* counterparts. The expression of CD31 largely surrounded the nuclei between the adjacent endothelial cells (Figure 4f). Cross-sectional views of an endothelialized PDMS

tube stained with CD31/nuclei (Figure 4g) and confocal 3D reconstruction image (Figure 4h) clearly confirmed the complete, intact lining of the HUVECs along the lumen.

To demonstrate the transport capability of the PDMS vessels, multiple organs-on-chips devices were connected as an integrated platform using the endothelialized PDMS tubes. Figure 5a shows an extendable, compact, and portable microfluidic circuit consisting of several bioreactors (on-chip organ module),[37] PDMS vascular tubes (ID: 0.64 mm), a flow meter, a medium reservoir, and a peristaltic pump. Six observation windows were arranged for fixing PDMS vessels (supplementary Figure S4). Those observation windows were used for microscopic observation of the endothelium in the PDMS vascular tubes. The flow direction is schematically illustrated in the inset of Figure 5a. The integrated system was designed to run constant medium perfusion sequentially from the medium reservoir to the mimic bioreactors resembling liver, heart, and lung through the PDMS vessel-based network.

To assess the bioactivity of the PDMS vessels, we monitored the concentration of ET-1 in the integrated system. The endothelial cell-derived ET-1 is known for its roles in vaso-activities, DNA synthesis, and proliferation of endothelial cells.[38] We demonstrated that, the secretion levels of ET-1 remained stable over a 14-day culture period (Figure 5b), indicating the viability and functionality of the endothelium. The platform itself could be further extended by adding extra modules such as additional organoids and sensors.

We subsequently investigated the suitability of the PDMS vessels as a vascular module to study drug effects. Specifically, we chose a panel of different drugs including anti-cancer drug doxorubicin (0-15 μg mL^{-1}), immunosuppressive drug rapamycin (0-10 μg mL^{-1}), and vasodilator medication minoxidil (0-5 μM), for evaluation. Doxorubicin has been reported to induce apoptosis of human endothelial cells starting from the lower μg mL^{-1} range.[39, 40] Rapamycin is a bacteria-derived agent possessing immunosuppressive activities, which have also been lately shown to induce endothelial cell death and thus is antiangiogenic.[41, 42] Minoxidil, a potent vasodilator usually used for the treatment of severe hypertension,[43] at higher doses may induce inhibitory effect on endothelial cells and also result in cardiovascular toxicity.[44] Evident from Figure 6b-d, the morphology of the HUVECs significantly altered to become rounded upon treatment of all three types of drugs for 12 h at their respective maximum concentrations tested, although the viability did not seem to decrease much compared to the control (Fig. 6a). Further quantifications of the secretion of vWF, a blood glycoprotein constantly produced by the endothelium,[45] from the PDMS vessels, showed a time- and dose-dependent reduction in response to the drugs (Figure 6e-g).

We further studied the NO production by the PDMS vessels upon treatment with several drug molecules. NO, synthesized by the nitric oxide synthases (NOSs) present in the vascular endothelial cells,[46] functions as an important mediator of numerous processes involved in the cardiovascular,[46] nervous,[47] and immune[48] systems. In the positive control, the traditionally recognized vasodilator histamine (100 μM)[49] spiked a drastic increase in the level of NO (approximately 190 nM) produced by the HUVECs in the PDMS vessels, which returned to the base level in approximately 5–10 min upon discharge of the agent (Figure

6h), indicating the active response of the endothelium. We then evaluated the effects of rapamycin (10 μg mL^{-1}), antiarrhythmic agent amiodarone (30 μM), and hepatotoxic drug acetaminophen (10 mM) on the NO production by the PDMS vessels. Rapamycin induced a sharp increase of the NO level (approximately 200 nM) similar to histamine treatment, which however, remained high over an extended period of time (Figure 6i). Amiodarone and acetaminophen treatments also resulted in elevated levels of NO synthesis (approximately 140 nM and 210 nM, respectively) by the endothelium, both of which rapidly decreased to the baseline within a few minutes (Figure 6j-k), in accordance with the reports in literature.[50], [51] Our drug studies with the endothelialized PDMS vessels revealed their biological functions, clearly indicating the advantages of these novel vascular organoids as individual modules for interconnecting multiple organs on chips.

Conclusions

In conclusion, we reported two simple and versatile templating strategies for fabricating elastomeric PDMS tubes with different diameters and wall thicknesses to emulate human blood vessels. These PDMS tubes could be further endothelialized to introduce the biological component, which was demonstrated to be functional and responsive to drug challenges. Therefore, the PDMS vascular tubes can integrate multiple organs-on-chip devices and may enable new mechanistic insights into organ-specific diseases and effects of exposures to biological and chemical insults. Our approach provides a more *in vivo*-resembling alternative for assembling the human organs-on-chips platforms, rather than the use of commercially available plastic tubes or conventional bulk vasculature chips.

Supplementary Material

Refer to Web version on PubMed Central for supplementary material.

Acknowledgments

The authors gratefully acknowledge funding by the Defense Threat Reduction Agency (DTRA) under Space and Naval Warfare Systems Center Pacific (SSC PACIFIC) Contract No. N6601-13-C-2027. The authors also acknowledge funding from the Office of Naval Research Young National Investigator Award, the National Institutes of Health (EB012597, AR057837, DE021468, HL099073, R56AI105024), and the Presidential Early Career Award for Scientists and Engineers (PECASE). W.Z. acknowledges funding from China's 1,000 Young Talents Program, Shanghai Young Eastern Scholar, Shanghai Pujiang Program (14PJ1404300), and NSFC (31501555). The publication of this material does not constitute approval by the government of the findings or conclusions herein.

References

1. Huh D, Torisawa Y-s, Hamilton GA, Kim HJ, Ingber DE. Lab Chip. 2012; 12:2156–2164. [PubMed: 22555377]
2. Moraes C, Mehta G, Lesher-Perez SC, Takayama S. Ann. Biomed. Eng. 2012; 40:1211–1227. [PubMed: 22065201]
3. Wikswo JP, Curtis EL, Eagleton ZE, Evans BC, Kole A, Hofmeister LH, Matloff WJ. Lab Chip. 2013; 13:3496–3511. [PubMed: 23828456]
4. Young EWK. Integr. Biol. 2013; 5:1096–1109.
5. Polini A, Prodanov L, Bhise NS, Manoharan V, Dokmeci MR, Khademhosseini A. Expert Opin Drug Discov. 2014; 9:335–352. [PubMed: 24620821]
6. Wikswo JP. Exp. Biol. Med. 2014; 239:1061–1072.

7. Esch EW, Bahinski A, Huh D. Nature Reviews Drug Discovery. 2015; 14:248–260. [PubMed: 25792263]
8. Zhang YS, Khademhosseini A. Nanomedicine. 2015; 10:685–688. [PubMed: 25816872]
9. Huh D, Hamilton GA, Ingber DE. Trends Cell Biol. 2011; 21:745–754. [PubMed: 22033488]
10. Rouwkema J, Gibbs S, Lutolf MP, Martin I, Vunjak-Novakovic G, Malda J. J. Tissue Eng. Regen. Med. 2011; 5:e164–e167. [PubMed: 21774080]
11. Bhatia SN, Ingber DE. Nat. Biotechnol. 2014; 32:760–772. [PubMed: 25093883]
12. Yum K, Hong SG, Healy KE, Lee LP. Biotechnology journal. 2014; 9:16–27. [PubMed: 24357624]
13. Shin M, King K, Matsuda K, Ishii O, Terai H, Weinberg E, Kaazempur-Mofrad M, Borenstein J, Detmar M, Vacanti J. Biomed Microdevices. 2006; 8:271–271.
14. Kim Y, Lobatto ME, Kawahara T, Lee Chung B, Mieszawska AJ, Sanchez-Gaytan BL, Fay F, Senders ML, Calcagno C, Becraft J, Tun Saung M, Gordon RE, Stroes ESG, Ma M, Farokhzad OC, Fayad ZA, Mulder WJM, Langer R. Proceedings of the National Academy of Sciences. 2014; 111:1078–1083.
15. Zhou J, Niklason LE. Integrative Biology. 2012; 4:1487–1497. [PubMed: 23114826]
16. Zheng W, Jiang B, Wang D, Zhang W, Wang Z, Jiang X. Lab on a Chip. 2012; 12:3441–3450. [PubMed: 22820518]
17. Bertassoni LE, Cecconi M, Manoharan V, Nikkhah M, Hjortnaes J, Cristino AL, Barabaschi G, Demarchi D, Dokmeci MR, Yang Y, Khademhosseini A. Lab Chip. 2014; 14:2202–2211. [PubMed: 24860845]
18. Liu M-C, Shih H-C, Wu J-G, Weng T-W, Wu C-Y, Lu J-C, Tung Y-C. Lab Chip. 2013; 13:1743–1753. [PubMed: 23475014]
19. Carola, R.; Harley, JP.; Noback, CR. Human anatomy and physiology. McGraw-Hill College; 1992.
20. Tien J. Curr. Opin. Chem. Eng. 2014; 3:36–41.
21. Wang X-Y, Pei Y, Xie M, Jin Z-H, Xiao Y-S, Wang Y, Zhang L-N, Li Y, Huang W-H. Lab Chip. 2015; 15:1178–1187. [PubMed: 25565271]
22. McDonald JC, Whitesides GM. Acc. Chem. Res. 2002; 35:491–499. [PubMed: 12118988]
23. Sia SK, Whitesides GM. Electrophoresis. 2003; 24:3563–3576. [PubMed: 14613181]
24. Tolle DA, Frye CL, Lehmann RG, Zwick TC. Sci. Total Environ. 1995; 162:193–207.
25. Armentano RL, Barra JG, Levenson J, Simon A, Pichel RH. Circulation Research. 1995; 76:468–478. [PubMed: 7859392]
26. Barra JG, Armentano RL, Levenson J, Fischer EI, Pichel RH, Simon A. Circulation Research. 1993; 73:1040–1050. [PubMed: 8222076]
27. Cox RH. Regional variation of series elasticity in canine arterial smooth muscles. 1978
28. Bank AJ, Wang H, Holte JE, Mullen K, Shammas R, Kubo SH. Circulation. 1996; 94:3263–3270. [PubMed: 8989139]
29. APTER JT. Circulation Research. 1967; 21:901–918. [PubMed: 6078150]
30. Fishbein GA, Fishbein MC. Arch. Pathol. Lab. Med. 2009; 133:1309. [PubMed: 19653731]
31. Zeitler, E. Radiology of Peripheral Vascular Diseases. Springer; 2000. p. 19-28.
32. Lee JN, Jiang X, Ryan D, Whitesides GM. Langmuir. 2004; 20:11684–11691. [PubMed: 15595798]
33. Zhang W, Choi DS, Nguyen YH, Chang J, Qin L. Sci. Rep. 2013; 3
34. Zhang W, Kai K, Choi DS, Iwamoto T, Nguyen YH, Wong H, Landis MD, Ueno NT, Chang J, Qin L. Proceedings of the National Academy of Sciences. 2012; 109:18707–18712.
35. Toworfe GK, Composto RJ, Adams CS, Shapiro IM, Ducheyne P. Journal of Biomedical Materials Research Part A. 2004; 71A:449–461. [PubMed: 15481053]
36. Annabi N, Selimovic S, Acevedo Cox JP, Ribas J, Afshar Bakooshli M, Heintze D, Weiss AS, Cropek D, Khademhosseini A. Lab on a Chip. 2013; 13:3569–3577. [PubMed: 23728018]
37. Bhise NS, Manoharan V, Massa S, Tamayol A, Ghaderi M, Miscuglio M, Lang Q, Zhang YS, Shin SR, Calzone G, Annabi N, Shupe T, Bishop C, Atala A, Dokmeci MR, Khademhosseini A. Biofabrication. 2016; 8:014101. [PubMed: 26756674]
38. Masaki T. Trends Pharmacol. Sci. 2004; 25:219–224. [PubMed: 15063086]

39. Lorenzo E, Ruiz-Ruiz C, Quesada AJ, Hernández G, Rodríguez A, López-Rivas A, Redondo JM. J. Biol. Chem. 2002; 277:10883–10892. [PubMed: 11779855]
40. Kalyanaraman, B.; Joseph, J.; Kalivendi, S.; Wang, S.; Konorev, E.; Kotamraju, S. Oxygen/ Nitrogen Radicals: Cell Injury and Disease. Springer; 2002. p. 119-124.
41. Bruns CJ, Koehl GE, Guba M, Yezhelyev M, Steinbauer M, Seeliger H, Schwend A, Hoehn A, Jauch K-W, Geissler EK. Clin. Cancer. Res. 2004; 10:2109–2119. [PubMed: 15041732]
42. Guba M, von Breitenbuch P, Steinbauer M, Koehl G, Flegel S, Hornung M, Bruns CJ, Zuelke C, Farkas S, Anthuber M, Jauch K-W, Geissler EK. Nat. Med. 2002; 8:128–135. [PubMed: 11821896]
43. Pettinger WA. New Engl. J. Med. 1980; 303:922–926. [PubMed: 6997744]
44. Hernández-Galilea E, Barahona JM, Vázquez R, Castro R, Urrutia M, Sánchez F. Archivos de la Sociedad Espanola de Oftalmologia. 2002; 77:361–368. [PubMed: 12098807]
45. Sadler JE. Annu. Rev. Biochem. 1998; 67:395–424. [PubMed: 9759493]
46. Palmer RMJ, Ashton DS, Moncada S. Nature. 1988; 333:664–666. [PubMed: 3131684]
47. Bredt DS, Snyder SH. Neuron. 1992; 8:3–11. [PubMed: 1370373]
48. Bogdan C. Nat. Immunol. 2001; 2:907–916. [PubMed: 11577346]
49. Lantoine F, Iouzalen L, Devynck MA, Millanvoye-Van Brussel E, David-Dufilho M. Biochem. J. 1998; 330:695–699. [PubMed: 9480877]
50. Uysal A, Azak S, Colak MC, Burma O, Ozguler IM, Ustundag B, Bayar MK. Biomedical Research. 2013; 24:486–492.
51. Gardner CR, Heck DE, Yang CS, Thomas PE, Zhang X-J, DeGeorge GL, Laskin JD, Laskin DL. Hepatology. 1998; 27:748–754. [PubMed: 9500703]

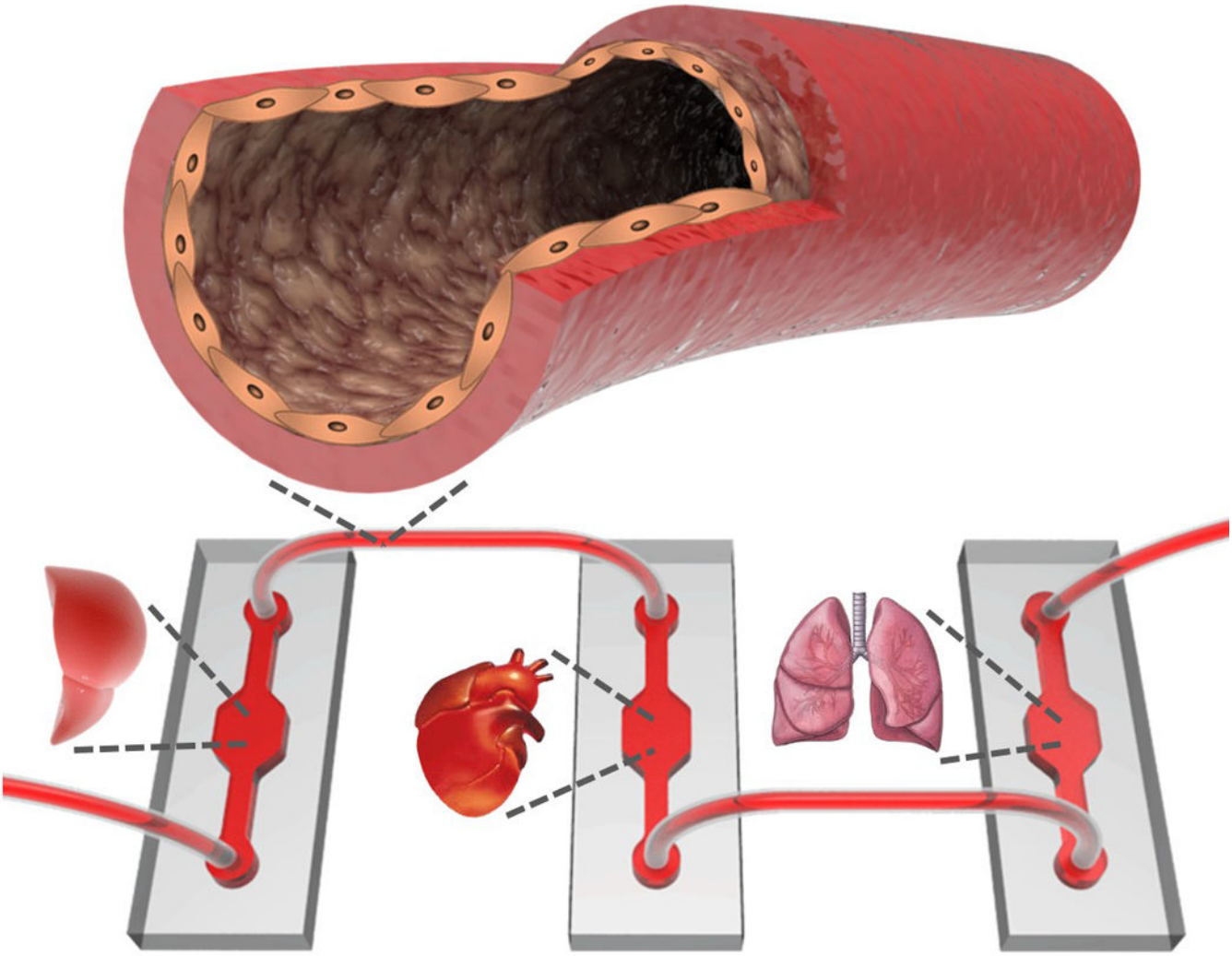

Fig. 1.

Schematic showing the concept of elastomeric endothelialized blood vessels for interconnecting multiple organs on chip systems (e.g. liver, heart, and lung modules as illustrated).

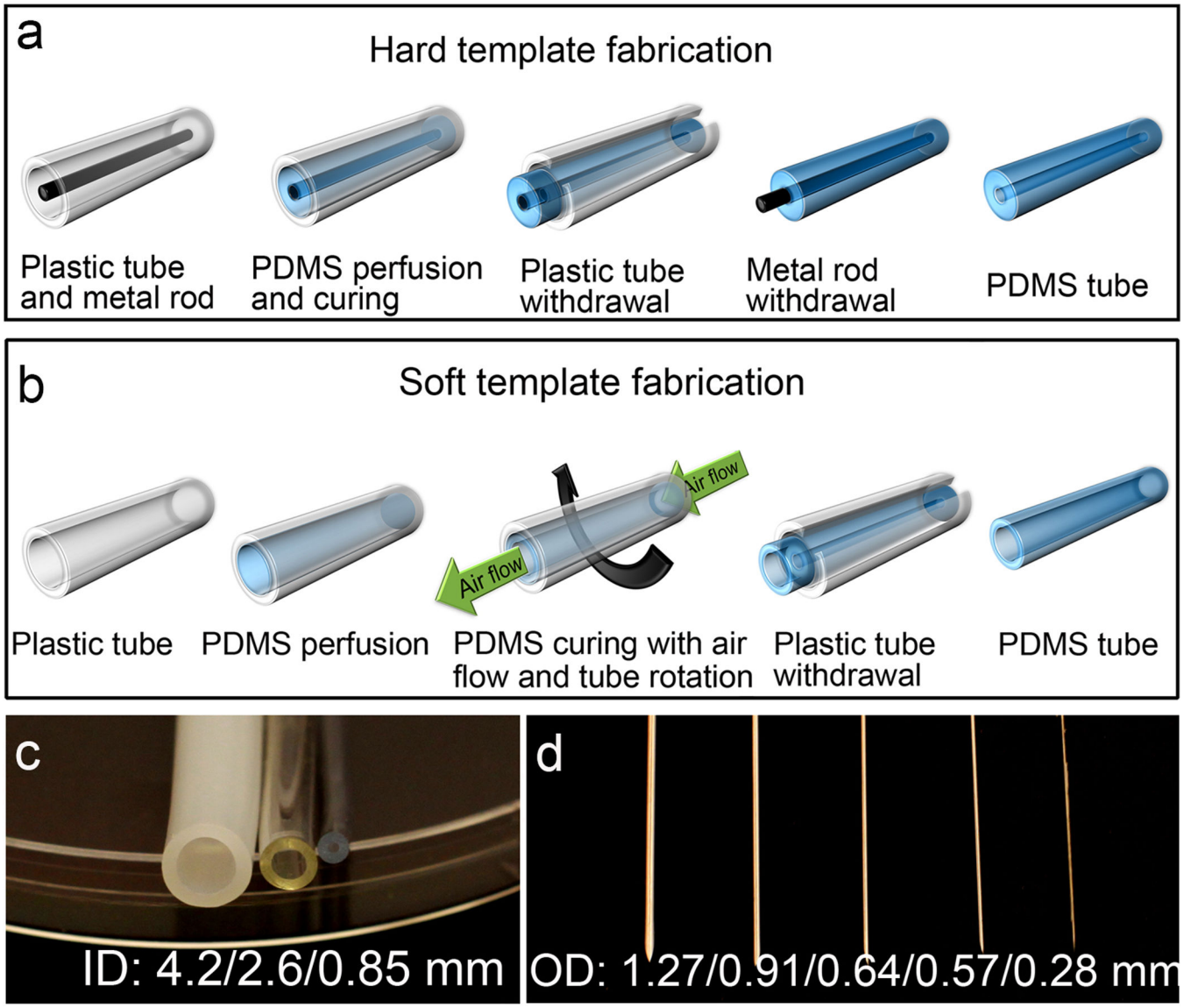

Fig. 2.

Templating strategies for fabrication of PDMS tubes. (a, b) Schematics of (a) hard templating and (b) soft templating approaches. (c) Photograph of the outer templating plastic tubes used in both the hard and soft templating methods. (d) Photograph of the metal rods/needles that are used as the inner templates in the hard templating method.

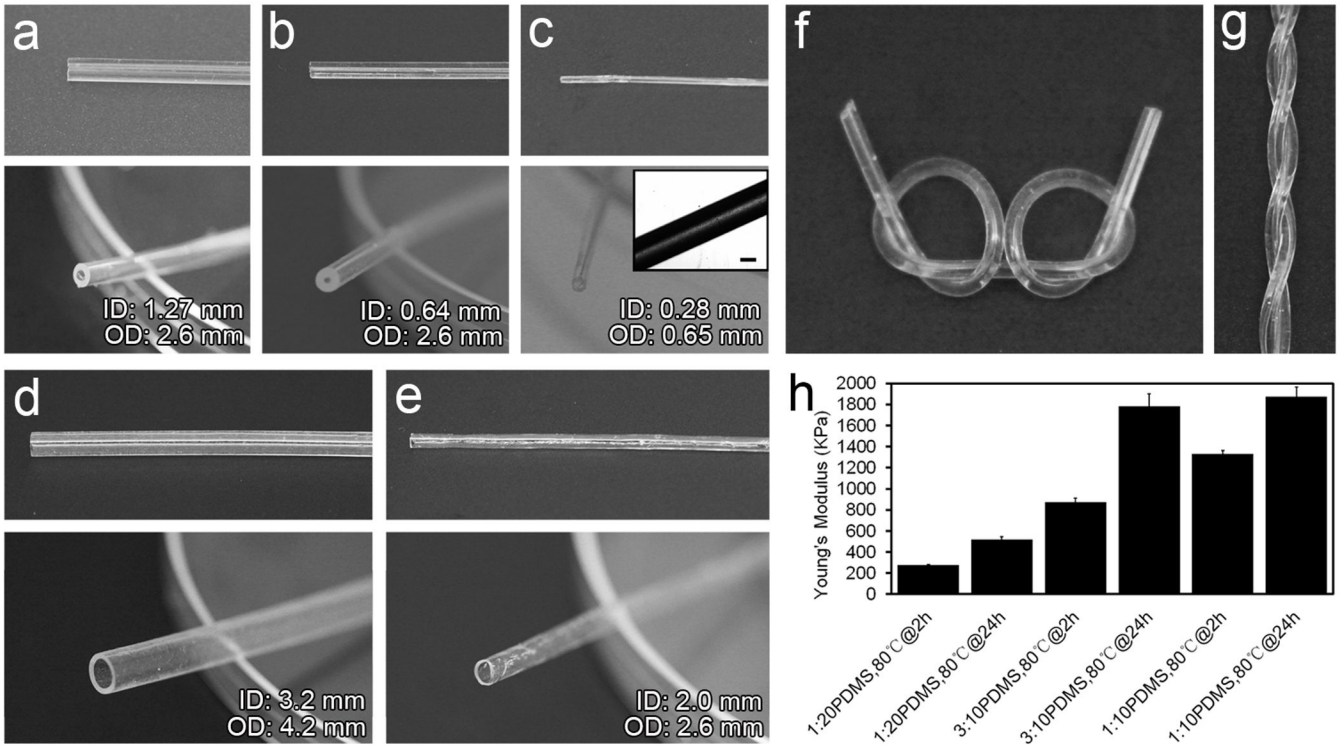

Fig. 3.

Properties of the PDMS tubes. (a-c) Photographs of fabricated PDMS tubes using the hard templating method. The inset in (c) is a 2.5X optical microscope image in which the scale bar is 500 μm. (d-e) Photographs of fabricated PDMS tubes using the soft templating method. (f-g) Twisting of the PDMS tubes. (h) Young's moduli of the PDMS material with different compositions and curing conditions.

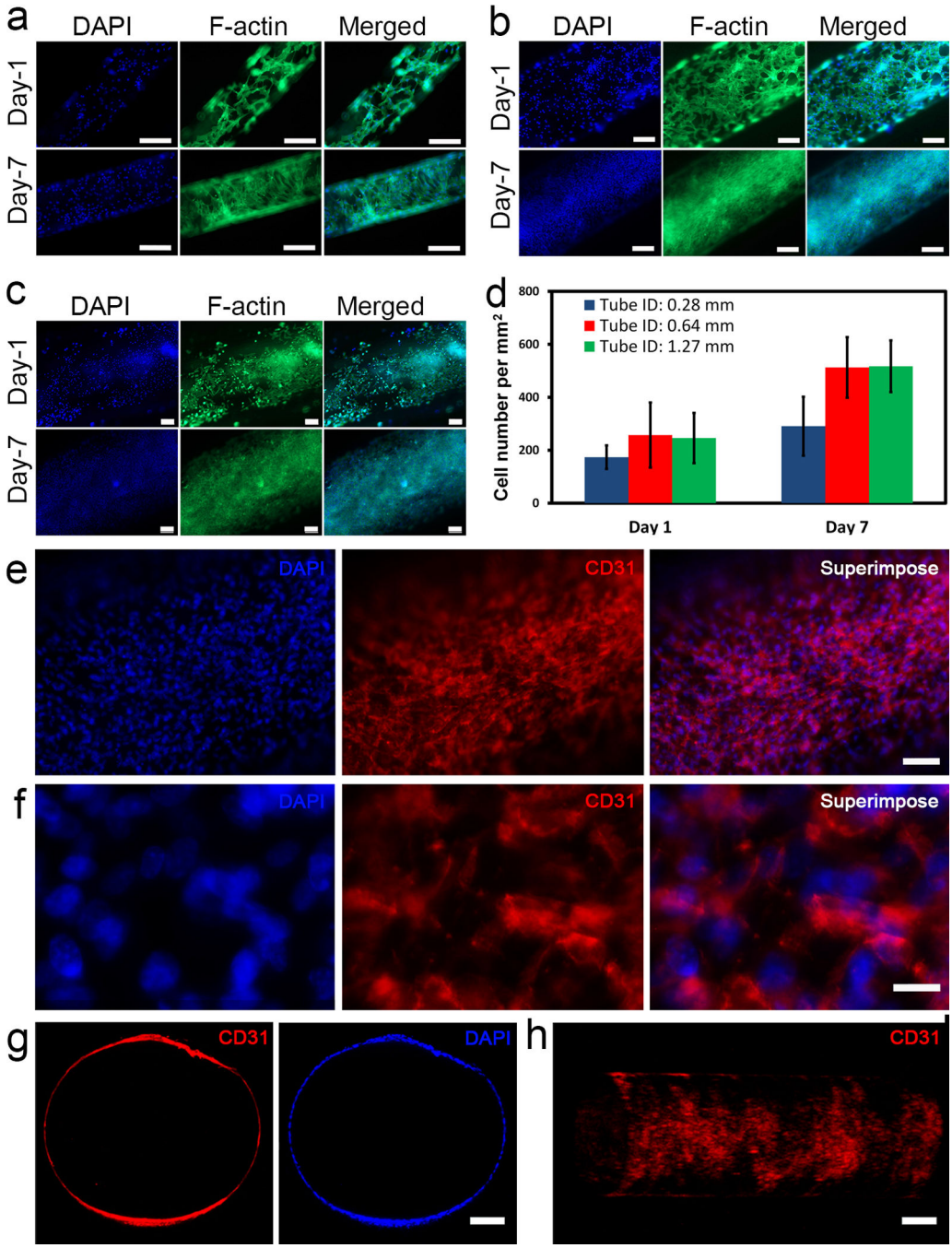

Fig. 4.

Endothelialization of the PDMS tubes. (a-c) Representative fluorescence micrographs showing HUVECs on the interior of the PDMS tubes with inner diameters of (a) 0.28 mm, (b) 0.64 mm, and (c) 1.27 mm at Day 1 and Day 7 of culture. F-actin and DAPI staining was performed to visualize the cytoskeleton and the nuclei and of cells. Scale bars: 200 μm. (d) Proliferation of HUVECs in the PDMS tubes. (e, f) Fluorescence micrograph of CD31- and DAPI-stained HUVECs in the PDMS tubes. (g) Confocal fluorescence micrographs of the cross-section of an endothelialized PDMS tube. Scale bar: 100 μm. (h) Confocal

reconstruction image showing the complete lumen formed by the HUVECs inside the PDMS tube. Scale bar: 200 μm.

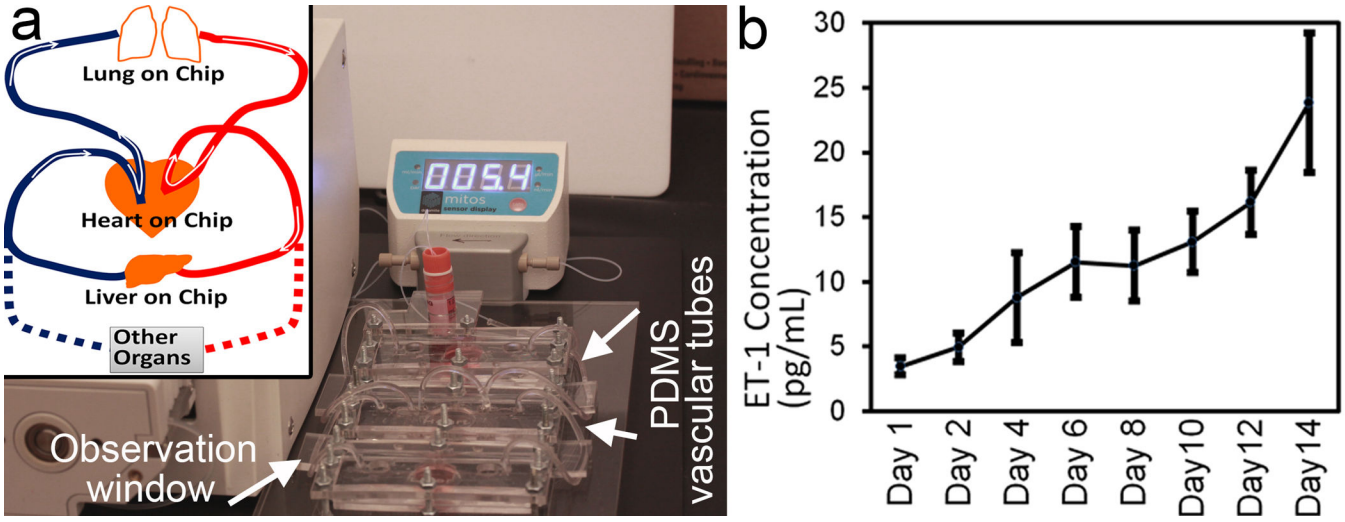

Fig. 5.

Endothelialized PDMS vessels for interconnection of multiple organ modules. (a) Photograph showing the assembly of the integrated multi-organ-on-chips platform including a medium reservoir, PDMS vascular tubes, three bioreactors mimicking the on-chip organ modules, and a flow meter, where the medium was circulated using a peristaltic pump. Inset: schematic of the designed multiple organs on chips system. (b) ET-1 secretion by the HUVECs in the PDMS tubes connecting multiple mimic organ modules.

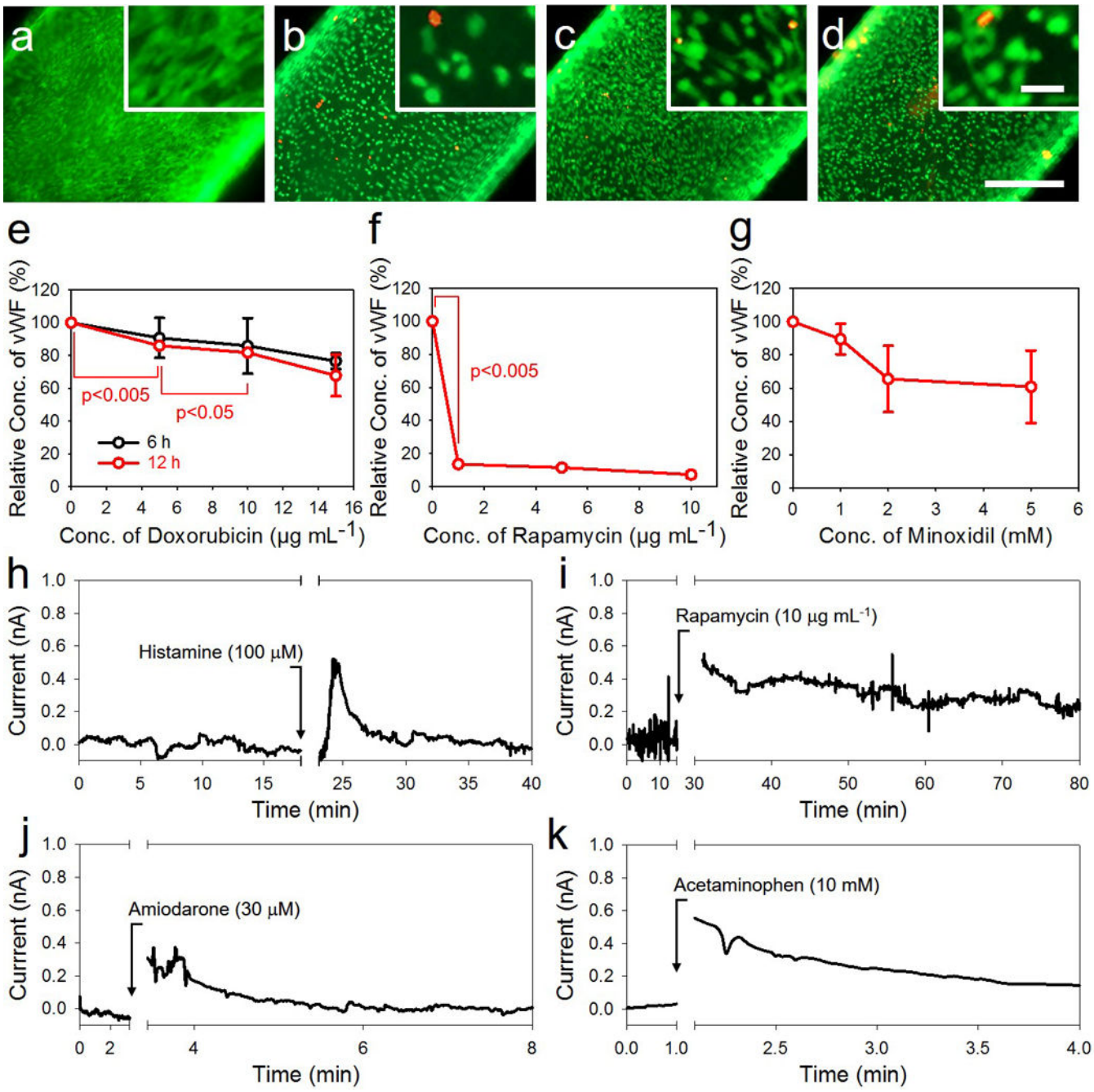

Fig. 6.

Biological responses of the endothelialized PDMS vessels upon drug treatment. (a-d) Live/dead images of the HUVECs inside the PDMS vascular tubes post treatment with (a) no drug, (b) 15 μg mL^{-1} doxorubicin, (c) 10 μg mL^{-1} rapamycin, and (d) 5 mM minoxidil for 12 h; scale bar: 500 μm. The insets are magnified images showing the morphologies of the HUVECs; scale bar: 50 μm. (e-g) Relative vWF secretion by the HUVECs inside the PDMS vascular tubes post treatment with doxorubicin, rapamycin, and minoxidil for 6 h and 12 h. (h) Levels of NO produced by the HUVECs inside the PDMS vascular tubes upon transient stimulation with 100 μM histamine (positive control), where a large spike of up to

approximately 190 nM NO was produced immediately post treatment. (i-k) Amperograms corresponding to NO levels produced by the HUVECs inside the PDMS vascular tubes upon transient stimulation with 10 μg mL^{-1} rapamycin, 30 μM amiodarone, and 10 mM acetaminophen.